Analyses of bifurcation of reaction pathways on a global reaction route map: A case study of gold cluster Au5

Yu Harabuchi, Yuriko Ono, Satoshi Maeda, and Tetsuya Taketsugu

Citation: The Journal of Chemical Physics **143**, 014301 (2015); doi: 10.1063/1.4923163
View online: http://dx.doi.org/10.1063/1.4923163
View Table of Contents: http://scitation.aip.org/content/aip/journal/jcp/143/1?ver=pdfcov
Published by the AIP Publishing

Analyses of bifurcation of reaction pathways on a global reaction route map: A case study of gold cluster Au_5

Yu Harabuchi,[1,2] Yuriko Ono,[1] Satoshi Maeda,[1,2] and Tetsuya Taketsugu[1,2,a)]
[1]*Department of Chemistry, Faculty of Science, Hokkaido University, Sapporo 060-0810, Japan*
[2]*CREST, Japan Science and Technology Agency, Tokyo 102-8666, Japan*

(Received 31 March 2015; accepted 17 June 2015; published online 1 July 2015)

A global reaction route map is generated for Au_5 by the anharmonic downward distortion following method in which 5 minima and 14 transition states (TSs) are located. Through vibrational analyses in the $3N - 7$ ($N = 5$) dimensional space orthogonal to the intrinsic reaction coordinate (IRC), along all the IRCs, four IRCs are found to have valley-ridge transition (VRT) points on the way where a potential curvature changes its sign from positive to negative in a direction orthogonal to the IRC. The detailed mechanisms of bifurcations related to the VRTs are discussed by surveying a landscape of the global reaction route map, and the connectivity of VRT points and minima is clarified. Branching of the products through bifurcations is confirmed by *ab initio* molecular dynamics simulations starting from the TSs. A new feature of the reaction pathways, *unification*, is found and discussed. © *2015 AIP Publishing LLC.* [http://dx.doi.org/10.1063/1.4923163]

I. INTRODUCTION

For an elementary reaction process, the intrinsic reaction coordinate (IRC)[1] is defined as the steepest descent path in mass-weighted coordinates on a potential energy surface (PES), starting from a transition state (TS) geometry in both positive and negative directions of the imaginary-frequency normal mode. For multiple-product reactions, the reaction mechanism can be understood as complex reactions composed of several elementary reactions in parallel reactions, consecutive reactions, or the mixture of them. In theoretical analyses of chemical reactions, the IRC plays a very important role to clarify the reaction mechanism.

Ohno and Maeda have developed a global search method for reaction pathways, named as anharmonic downward distortion following (ADDF), which has made it possible to find many TSs starting from one minimum structure on the PES.[2–4] A concept of global reaction route mapping (GRRM) has been established as the approach to explore chemical reaction pathways automatically through a combination of ADDF and IRC computations. In this paper, the "global map" stands for a map of IRC paths obtained by the ADDF method. Further details of the ADDF method are described in recent reviews.[5,6] Moreover, Maeda and Morokuma developed a new methodology to locate a TS geometry for A + B type reactions, named as artificial force induced reaction (AFIR),[7] which has made possible applications of GRRM more extensively. In 2014, the target of AFIR is extended to finding TSs of intramolecular reactions.[8]

There is a case where two different products are generated from a single TS. This is a case of bifurcation of the reaction pathway.[9–15] Very recently, trifurcation of the reaction pathway was reported,[16] which suggests the existence of multi-branching reaction pathway. The IRC itself follows a steepest descent direction on the PES, and thus, it does not bifurcate, indicating that the other pathway leading to another product is missed in IRC calculations. The relation of a reaction coordinate and bifurcation was discussed in detail from a viewpoint of geometrical symmetry.[17] When a reaction pathway has a branching point on the way, there should appear a ridge between the branching pathways.[18] Valtazanos and Ruedenberg introduced a name of *valley-ridge inflection* (VRI) point to represent the point where the potential curvature with respect to a transverse vibrational coordinate turns its sign from positive to negative along the IRC.[9] Basilevsky discussed a mathematical aspect of the structural stability and branching points on the IRC.[19] Quapp[20] discussed valley-ridge border lines on multi-dimensional PESs and proposed a mathematical definition of VRI that needs to fulfill two conditions: (i) one eigenvalue of the Hessian matrix is zero and (ii) the energy gradient is orthogonal to the corresponding eigenvector of zero eigenvalue. From this definition, the points where the shape of PES changes from a valley to a ridge on the IRC do not satisfy these conditions in general, and a new concept, *valley-ridge transition* (VRT) point, was introduced to represent the point where a geometrical feature of the potential energy variation in a direction of the transverse vibrational mode orthogonal to the IRC changes from valley to ridge.[21] Following this definition, "VRT" is used throughout in the present paper. The occurrence of the reaction path branching can be examined by checking appearance of VRT points along the IRCs.

The VRT points on the IRC are classified according to the symmetry of the corresponding vibrational mode. When the vibrational mode with VRT is a non-totally symmetric mode, the reaction path bifurcates into right-hand and left-hand geometries that are symmetrically equivalent to each other. In this case, if the ridge feature of the IRC is conserved at the terminal point, this terminal is not a minimum but a transition state that connects symmetrically equivalent minima. This type

a)Author to whom correspondence should be addressed. Electronic mail: take@sci.hokudai.ac.jp

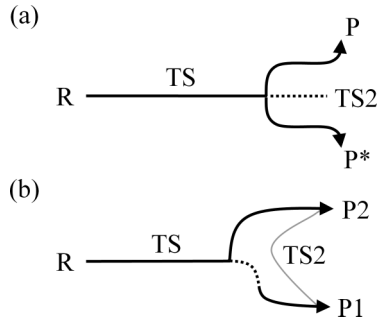

FIG. 1. Schematic pictures of a classification of bifurcation mechanism based on the symmetry of the vibrational mode with VRT: (a) non-totally symmetric VRT and (b) totally symmetric VRT. R and TS denote a reactant and a transition state, respectively. P and P* denote symmetrically equivalent product minima, while P1 and P2 denote product minima of different type to each other. TS2 is the second transition state that connects (a) P and P* or (b) P1 and P2. The dotted line indicates a ridge path.

of reaction pathways could be found through IRC analyses, and so, there have been a number of theoretical studies on such non-totally symmetric VRT.[9–14,18,22–25] On the other hand, when the vibrational mode with VRT is a totally symmetric mode, the reaction pathway bifurcates asymmetrically, and the products with different types are expected from the bifurcating reaction pathways. In this case, however, it is difficult to notice an occurrence of totally symmetric VRT since the IRC should terminate at one of product minima via a ridge-valley transition (RVT) point. Therefore, only a small number of reactions have been reported as the case of totally symmetric VRT.[26–34] The difference of non-totally symmetric and totally symmetric VRTs is schematically shown in Fig. 1.

An appearance of VRT points along the IRC suggests the existence of additional product minima that are connected from a region of VRT points. VRT points can be found by computing frequencies of transverse vibrational modes along the IRC,[10] but there is no way to follow the pathway from a VRT point to the additional product minima only based on geometrical feature of the PES. Dynamics simulations were sometimes employed to examine branching ratios over several products for bifurcating reactions in previous studies.[28,30–32]

To our knowledge, all previous studies have focused on the specific IRC that accompanies VRT. In the present study, the bifurcation analyses of the IRC are combined with GRRM computations, and the appearance of VRT in the global reaction route map and the connection of VRT with additional product minimum are examined for a small gold cluster, Au_5. Since the pioneer work of Haruta *et al.*,[35] gold clusters have been paid attention extensively[36–38] due to a large interest in its unique catalytic activity. Au_5 is a very interesting species as a target because plural symmetrically equivalent paths exist due to a high symmetry of the system. All of the connections of the reaction pathways with a branching nature are examined based on geometrical similarities for a pair of IRCs.

II. COMPUTATIONAL DETAILS

The ADDF method[2–6] is applied to a global search for minima (MINs) and TSs of Au_5. The IRC pathways are simultaneously determined for the respective TSs without symmetry restriction. The occurrences of the VRTs are examined by calculating frequencies of transverse vibrational modes orthogonal to the reaction path. For N atomic system, $3N - 7$ transverse vibrational modes are calculated as functions of a reaction coordinate, s, from diagonalization of the projected Hessian matrices as[10,39,40]

$$\left((\mathbf{1} - \sum_{j=1}^{7} \mathbf{v}_j \mathbf{v}_j^{\mathrm{t}})\mathbf{H}(s)(\mathbf{1} - \sum_{j=1}^{7} \mathbf{v}_j \mathbf{v}_j^{\mathrm{t}})\right)\mathbf{L}_i(s) = \lambda_i(s)\mathbf{L}_i(s), \quad (1)$$

where $\mathbf{H}(s)$, $\mathbf{L}_i(s)$, and $\lambda_i(s)$ are the Hessian matrix, the ith vibrational mode (eigenvector), and the ith eigenvalue at s, and $\mathbf{v}_i$ denotes the ith unit vector for three translational modes, three rotational modes, and the reaction-path tangent. The vibrational frequency for each transverse mode, ν_i, is calculated in wavenumber as

$$\nu_i(s) = \frac{\sqrt{\lambda_i(s)}}{2\pi c}, \quad (2)$$

where c is the speed of light. After passing a VRT point, the lowest ν_i becomes imaginary number (the corresponding λ_i becomes negative).

The appearance of VRT indicates the existence of two product minima, and thus, geometrical structure of each VRT could be similar to the structure of one of the TSs that connects the product minimum of a terminal of the IRC with VRT and the additional product minimum. In order to discuss connections between the VRT point and the additional product minima from this viewpoint, geometrical structures on the IRC accompanying VRT points are compared with those on the IRCs determined for the other TSs. The comparisons of geometrical structures are carried out by a distance matrix where all the interatomic distances are saved from the smallest to the largest one in one-dimensional array. It is noted that this representation cannot distinguish geometries of an enantiomer.

To verify the branching of products through VRT points from a dynamical viewpoint, we also carried out *ab initio* molecular dynamics (AIMD) simulations starting from TS for the IRCs that accompany VRT. The direction of initial velocities is determined randomly within internal degrees of freedom ($3N - 6 = 9$), and the initial kinetic energy was set as 5 kcal/mol. The number of trajectories is increased until 10 trajectories enter the product-side of branching nature.

The adiabatic potential energies, energy gradients, and Hessian matrices were calculated by the density functional theory (DFT) method with Perdew-Burke-Ernzerhof (PBE) functionals and LanL2DZ basis sets, with the Gaussian09 program package.[41] The ADDF search was performed by the GRRM11 program package,[42] while transverse vibrational frequency calculations were performed by the developmental version of GRRM.[43] AIMD simulations were performed by using a developmental version of SPPR program.[44]

III. RESULTS AND DISCUSSION

By combined ADDF and IRC calculations for Au_5, 5 minima and 14 transition-state structures are located on the potential energy surface. Figure 2 shows geometrical structures, relative energies, and point groups of these stationary

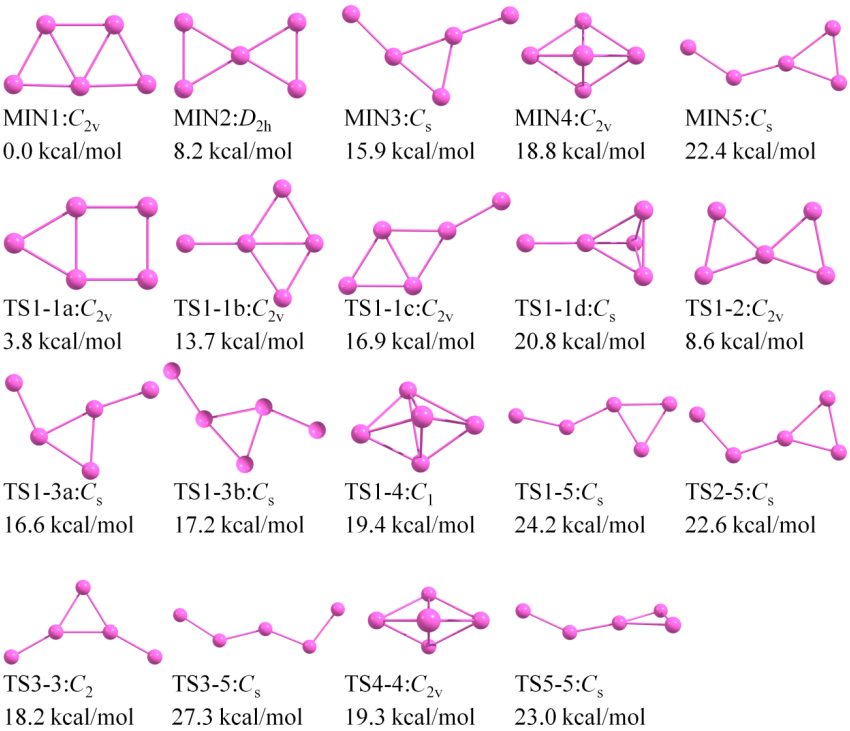

FIG. 2. All of the minima and TS structures for Au_5. The point group and the relative energy in kcal/mol are also given for each structure.

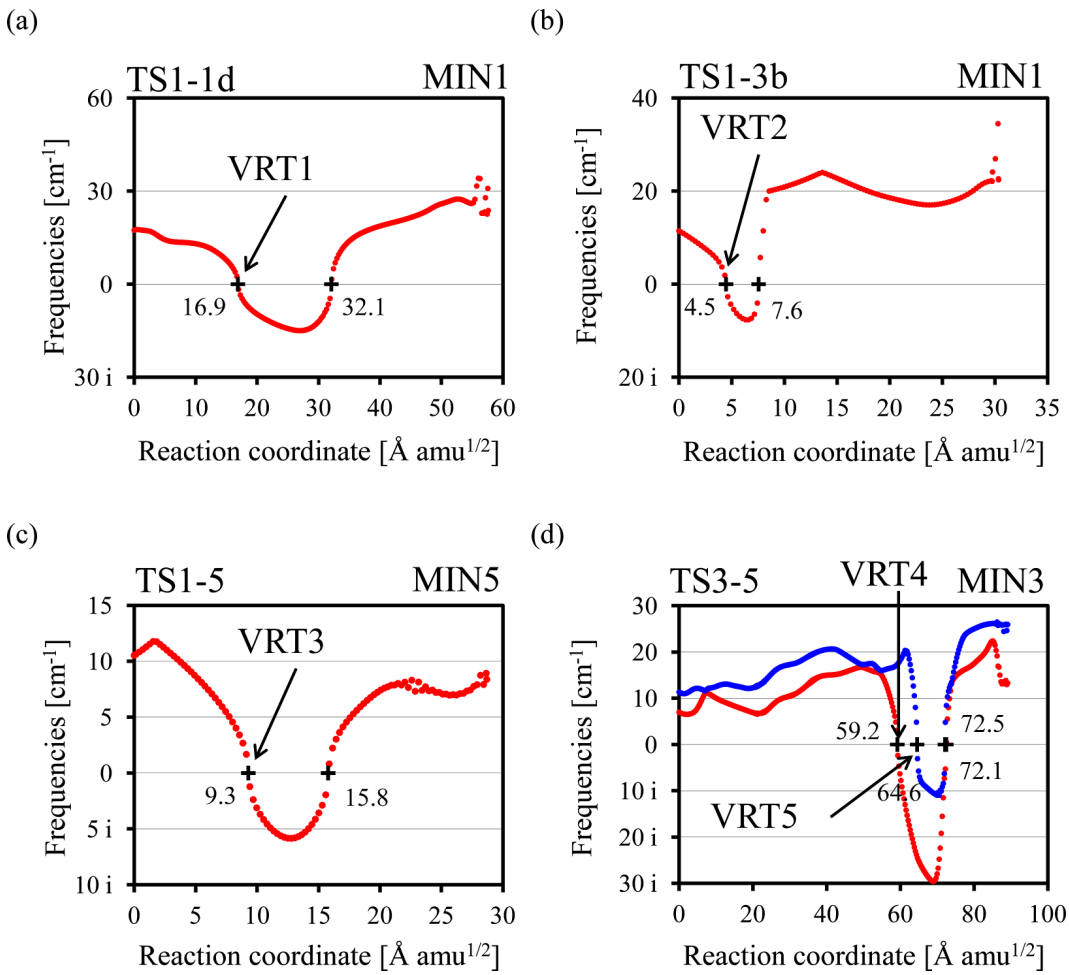

FIG. 3. Variations of the lowest vibrational frequencies for the transverse modes perpendicular to the IRC: (a) TS1-1d → MIN1, (b) TS1-3b → MIN1, (c) TS1-5 → MIN5, and (d) TS3-5 → MIN3. In case (d), the second lowest frequency is also shown. The VRT and ridge-valley transition (RVT) points are indicated by "+" with the reaction coordinate.

structures, MINn and TSn-m, where TSn-m denotes a transition state between MINn and MINm. As shown here, there are four distinguished transition states for a permutation of nuclei in MIN1, TS1-1a ~ TS1-1d, and two distinguished transition states between MIN1 and MIN3 and TS1-3a and TS1-3b. Most structures are a planar geometry because of relativistic effects of gold atoms.[45]

Next, VRT points are searched by calculating frequencies of transverse vibrational modes along all of the IRCs through diagonalization of the projected Hessian matrices, according to Eq. (1). Among 14 IRCs, four IRCs are found to have one or two VRT points on the way: TS1-1d → MIN1 (VRT1), TS1-3b → MIN1 (VRT2), TS1-5 → MIN5 (VRT3), and TS3-5 → MIN3 (VRT4 and VRT5). The vibrational frequencies of the transverse modes accompanying VRT are plotted in Fig. 3. As to the IRC from TS3-5 to MIN3, there appear two VRT points at a very close region as shown in Fig. 3(d).

Figure 4 shows the mechanism and the connection for the IRCs with VRT described above where MINs, TSs, and VRTs are depicted with relative energies and molecular geometries. The vibrational mode of an imaginary frequency is given for each TS, while the vibrational mode of zero frequency is given for each VRT. IRCs are shown by black solid lines, while molecular point groups are indicated by green dashed lines. In

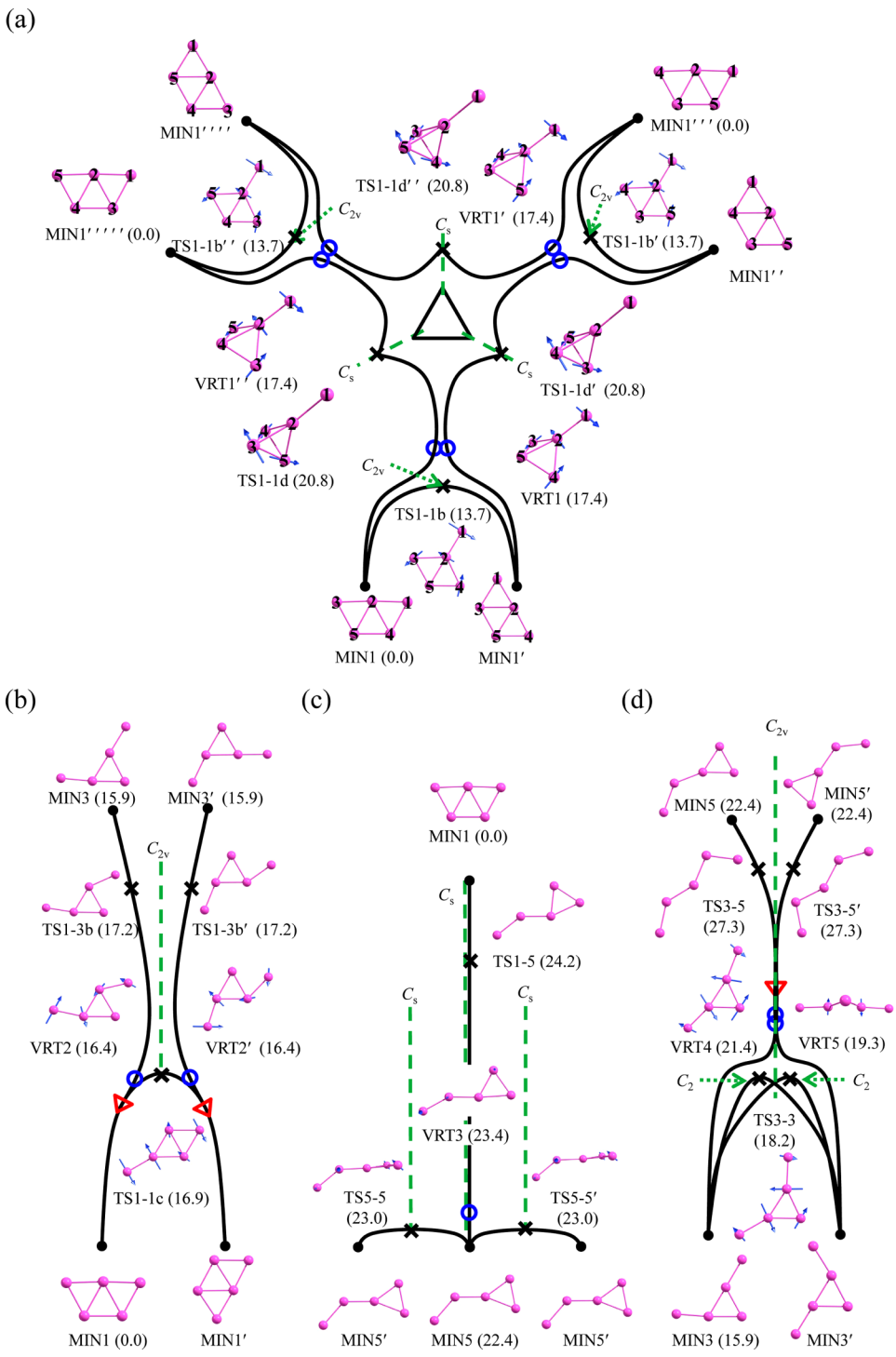

FIG. 4. Schematic pictures of reaction pathways with bifurcation for Au_5: (a) MIN1′′′′ → TS1-1d → MIN1/MIN1′, (b) MIN3 → TS1-3b → MIN1/MIN1′, (c) MIN1 → TS1-5 → MIN5/MIN5′, and (d) MIN5 → TS3-5 → MIN3/MIN3′. Molecular geometries of MIN, TS, and VRT are shown with relative energies in kcal/mol. Black solid lines denote IRC, while green dotted lines denote the symmetry plane. Black cross marks denote TS, blue circles denote VRT, and red triangles denote a unification point.

Fig. 4, the symmetrically equivalent IRCs are also depicted. In addition, the IRCs related to bifurcations caused by VRT are also shown. These additional IRCs are found through comparisons of geometries for all the pairs of IRCs, as described in Sec. II. It is interesting to note the similarity in geometry between the VRT and the closely lying TS. The relationship between a VRT and the corresponding TS is also confirmed by AIMD simulations. In the following, a detailed mechanism of the reaction-path branching is discussed on four cases shown in Fig. 4.

TS1-1d → VRT1 → MIN1/MIN1′ (Fig. 4(a)): The first case is an IRC that connects symmetrically equivalent minima, MIN1′′′′′ and MIN1, via TS1-1d. MIN1 is a global minimum with an isosceles trapezium form of C_{2v} symmetry, and there are 60 symmetrically equivalent minima for MIN1. In Figs. 4(a), six structures are involved. By distinguishing five gold atoms by number as shown in Fig. 4(a), MIN1, MIN1′, MIN1′′, MIN1′′′, MIN1′′′′, and MIN1′′′′′ can be represented by (123)(45), (124)(35), (125)(43), (124)(53), (123)(54), and (125)(34), respectively. TS1-1d has a pseudo-C_{3v} (C_s) structure, and the pure C_{3v}-geometry corresponds to a second-order saddle point; there exist three symmetry-reduced transition states: TS1-1d, TS1-1d′, and TS1-1d′′. In these TSs, the imaginary-frequency mode belongs to a non-totally symmetric mode, A′′, and thus, the IRC starting from TS1-1d belongs to C_1 symmetry. Then, a totally symmetric VRT1 appears on descending from TS1-1d to MIN1 as shown in Fig. 4(a). The VRT1 structure and the zero-frequency mode are similar to those at TS1-1b, and thus, it can be concluded that the VRT1 is related to the branching of MIN1 and MIN1′ via a TS1-1b. AIMD simulations show that, among 10 trajectories from TS1-1d, 7 trajectories lead to MIN1, while 3 trajectories lead to MIN1′. Thus, it is confirmed that the dynamical reaction pathways from TS1-1d branch to MIN1 and MIN1′ via VRT1. The branching ratio for MIN1 and MIN1′ is 7:3, indicating that the product, that is not the terminal of the IRC (MIN1′), is generated at the lower rate in this reaction.

TS1-3b → VRT2 → MIN1/MIN1′ (Fig. 4(b)): The second case is an IRC that connects MIN3 and MIN1 via TS1-3b. Starting from MIN3, the molecule conserves a planar geometry of C_s symmetry along the IRC, and after passing TS1-3b, a totally symmetric bifurcation occurs at VRT2 as shown in Fig. 4(b). It is very interesting to note that the IRC from TS1-3b combines with the IRC from TS1-1c just after passing VRT2. This feature can be referred to as *unification* of the reaction pathways, which is an opposite concept of *bifurcation*. The vibrational mode of zero-frequency at VRT2 shows a similar feature to the imaginary-frequency vibrational mode at TS1-1c as shown in Fig. 4(b). It is concluded that the VRT2 is related to the bifurcation into MIN1 and MIN1′ connected by TS1-1c. AIMD simulations show that among 10 trajectories from TS1-1c, 8 trajectories lead to MIN1, while 2 trajectories lead to MIN1′. The terminal of the IRC, MIN1, is preferred as a product from TS1-1c, because of the energy barrier between VRT2 and TS1-1c as shown in Fig. 4(b).

TS1-5 → VRT3 → MIN5/MIN5′ (Fig. 4(c)): The third case is an IRC that connects MIN1 and MIN5 via TS1-5. From MIN1 to MIN5, the molecule conserves C_s symmetry throughout along the IRC, and the out-of-plane mode of A′′ gets an imaginary frequency after passing VRT3 as shown in Fig. 4(c). This is a case of non-totally symmetric bifurcation, although the terminal of the IRC becomes a minimum, i.e., MIN5. The zero-frequency mode at VRT3 is related to the mode leading to MIN5′ through a rotation of the triangle of Au_3 fragment in Au_5. Since the energy difference between the VRT3 and TS5-5 is very small, 0.4 kJ/mol, it can be expected that a potential energy profile along the rotational motion of the Au_3 fragment is very flat, and the rotation can occur easily in the actual dynamics. AIMD simulations show that among 10 trajectories from TS1-5, the rotational motion of the triangle of Au_3 is observed in 7 trajectories, which invokes structural transformation between MIN5 and MIN5′. In this case, however, it is difficult to distinguish whether trajectories reach MIN5′ directly or via MIN5, because of a low energy barrier between MIN5 and MIN5′.

TS3-5 → VRT4 → MIN3/MIN3′ (Fig. 4(d)): The fourth case is an IRC that connects MIN5 and MIN3 via TS3-5. In this case, the molecule keeps C_s symmetry throughout along the IRC, but interestingly, the symmetry of the IRC becomes a higher symmetry, C_{2v}, in a limited region after passing TS3-5, which is a very rare phenomenon. The rise of molecular symmetry indicates *unification* of two reaction pathways of C_s symmetry, which actually occurs as shown in Fig. 4(d). Non-totally symmetric VRT4 (with respect to B_1 mode) and VRT5 (with respect to A_2 mode) appear in C_{2v}-IRC, and thus, this can be categorized as a non-totally symmetric bifurcation. In a strict sense, the C_{2v} symmetry of the IRC must be conserved and the terminal of C_{2v}-IRC should become a second-order saddle point (SOSP) with two imaginary frequency modes, but a numerically small deviation from C_{2v} should invoke a

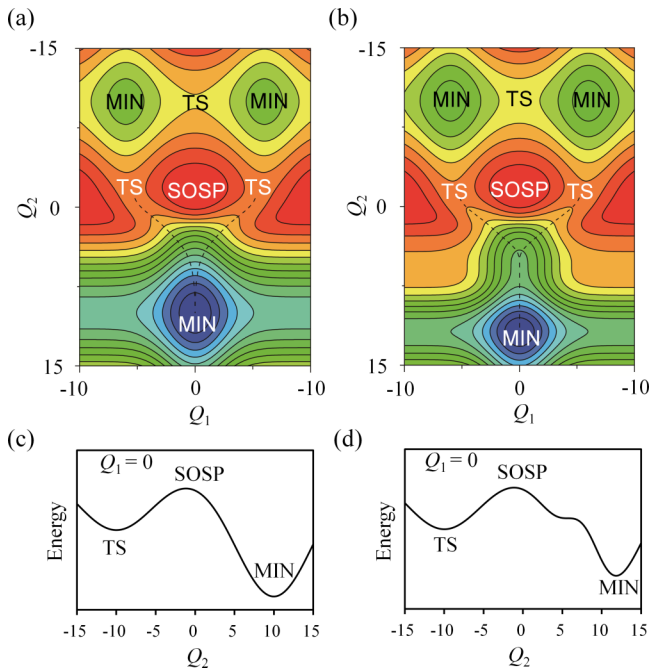

FIG. 5. Schematic two-dimensional model potential surfaces for discussions of the unification. Minima (MIN), TSs, and SOSP are involved. (a) and (b) show potential contour plots, while (c) and (d) show variations of the energy along the line of $Q_1 = 0$. Black dashed lines in (a) and (b) indicate the steepest descent pathways from two TSs.

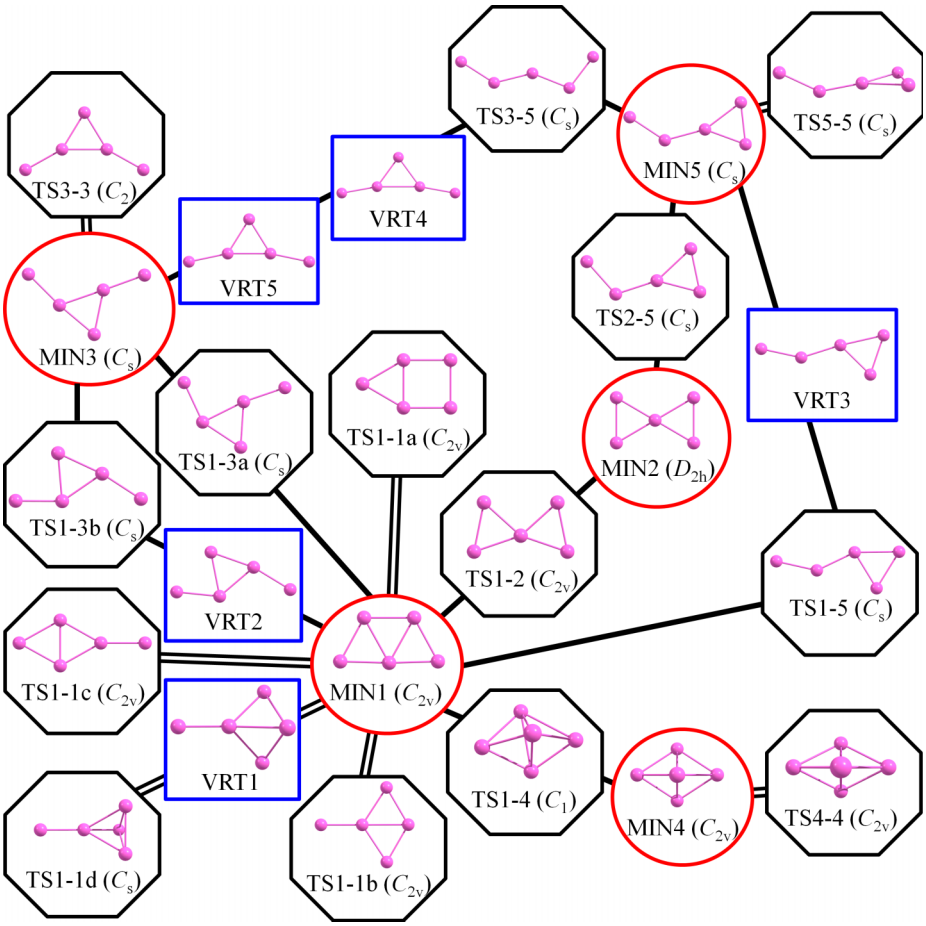

FIG. 6. The global reaction route map for Au_5. A circle node indicates minimum (MIN), an octagon node indicates TS, and a square node indicates VRT. A solid line indicates an IRC.

reduction of the symmetry of the IRC to C_s, which makes the terminal of the IRC MIN3 or MIN3′. This bifurcation is related to VRT4 of B_1 symmetry. It is interesting to note that TS3-3 that connects MIN3 and MIN3′ has an out-of-plane geometry with C_2 symmetry. The A_2 mode related to VRT5 should invoke a geometry change from the terminal of C_{2v}-IRC (SOSP) to TS3-3. AIMD simulations show that among 10 trajectories from TS3-5, 6 trajectories lead to MIN3, while 4 trajectories lead to MIN3′. In this case, MIN3 and MIN3′ are generated with almost the same rate, which can be expected for a non-totally symmetric bifurcation.

It is known that two IRCs cannot be unified except at stationary points from a mathematical definition of IRC and that the molecular symmetry cannot change along the IRC except at stationary points. In the second (Fig. 4(b)) and fourth (Fig. 4(d)) cases, however, unification of two reaction pathways (IRCs) is observed while descending on the PES, and also the molecular symmetry is raised from C_s to C_{2v} on the way in the fourth case. To get insights into the mechanism of unification and the symmetry-raising on the way, geometrical features of the PES were examined around the unification point, and it is found that the unification can occur around a shoulder region of the energy profile along the IRC. To illustrate this finding, two-dimensional model potentials are shown in Figs. 5(a) and 5(b) where each PES involves three minima (MIN), three TSs, and one SOSP, with dotted lines showing two steepest descent paths from TS to the lower MIN. The difference in Figs. 5(a) and 5(b) appears in a region between the SOSP and the lower MIN. The energy variations along the line of $Q_1 = 0$ are shown in Fig. 5(c) (corresponding to Fig. 5(a)) and Fig. 5(d) (corresponding to Fig. 5(b)). As shown here, there is a shoulder region between SOSP and MIN in Fig. 5(d), where two steepest descent lines from TSs come together and are unified. This shoulder-feature is a necessary condition for a unification of the reaction pathways.

Finally, the global reaction route map involving VRTs is shown in Fig. 6 where MINs are depicted by circle nodes, TSs are depicted by octagon nodes, and VRTs are depicted by square nodes. To avoid the complexity of the map, permutational isomers are not considered in Fig. 6. As shown in Figs. 4(a)-4(d), VRT1 is related to TS1-1b, VRT2 is related to TS1-1c, VRT3 is related to TS5-5, and VRT4 and VRT5 are related to TS3-3. Thus, four bifurcating reaction pathways in Au_5 are all categorized as a branch into permutational isomers, although both non-totally symmetric and totally symmetric cases are found.

IV. CONCLUDING REMARKS

The present study is the first attempt to locate all the VRT points in a global reaction route map and to clarify the branching products connected from the VRTs. The combined ADDF and IRC calculations are applied to a gold cluster, Au_5, using the GRRM program, and five minima and fourteen TSs are located. Through calculations of the projected Hessians along the reaction pathways for fourteen IRCs, four IRCs are found to have VRT points on the way. For each

case, the detailed branching mechanisms are discussed, and the connectivity of VRTs and product minima is clarified. It is found that each VRT has a strongly related TS leading to a branch into two product minima. The relationship between the VRT and the corresponding TS is confirmed by AIMD simulations. Through examinations of the reaction pathways on a global reaction route map, we have also found a new feature, unification of the reaction pathways, and examined the detailed mechanism. It is shown that, using the model potentials, a shoulder-feature of the PES along the IRC is a sign of the unification.

The concept of bifurcation is significant to understand the whole reaction mechanism for a given molecular system, and it is demonstrated that GRRM approach is a strong tool for discussions of the connectivity of the reaction pathways including bifurcations. The automated-search method to determine the connection of bifurcating pathways from a VRT to the product minima is under development.

ACKNOWLEDGMENTS

This work is partly supported by a grant from Japan Science and Technology Agency with a Core Research for Evolutional Science and Technology (CREST) in the Area of "Establishment of Molecular Technology towards the Creation of New Functions" at Hokkaido University. This work is supported in part by a grant from the Institute for Quantum Chemical Exploration (IQCE) and in part by a Grant-in-Aid for Scientific Research from the Ministry of Education, Culture, Sports, Science, and Technology. Y.O. thanks supports from the Japan Society for the Promotion of Science for Research Fellowships for Young Scientists. The computations were performed using the Research Center for Computational Science, Okazaki, Japan. The authors declare no competing financial interest.

[1]K. Fukui, J. Phys. Chem. **74**, 4161 (1970).
[2]K. Ohno and S. Maeda, Chem. Phys. Lett. **384**, 277 (2004).
[3]S. Maeda and K. Ohno, J. Phys. Chem. A **109**, 5742 (2005).
[4]K. Ohno and S. Maeda, J. Phys. Chem. A **110**, 8933 (2006).
[5]S. Maeda, K. Ohno, and K. Morokuma, Phys. Chem. Chem. Phys. **15**, 3683 (2013).
[6]S. Maeda, T. Taketsugu, K. Morokuma, and K. Ohno, Bull. Chem. Soc. Jpn. **87**, 1315 (2014).
[7]S. Maeda and K. Morokuma, J. Chem. Theory Comput. **7**, 2335 (2011).
[8]S. Maeda, T. Taketsugu, and K. Morokuma, J. Comput. Chem. **35**, 166 (2014).
[9]P. Valtazanos and K. Ruedenberg, Theor. Chim. Acta **69**, 281 (1986).
[10]J. Baker and P. M. W. Gill, J. Comput. Chem. **9**, 465 (1988).
[11]P. Valtazanos, S. T. Elbert, S. Xantheas, and K. Ruedenberg, Theor. Chim. Acta **78**, 287 (1991).
[12]T. Taketsugu, N. Tajima, and K. Hirao, J. Chem. Phys. **105**, 1933 (1996).
[13]T. Yanai, T. Taketsugu, and K. Hirao, J. Chem. Phys. **107**, 1137 (1997).
[14]T. Taketsugu, T. Yanai, K. Hirao, and M. S. Gordon, J. Mol. Struct.: THEOCHEM **451**, 163 (1998).
[15]S. Maeda, Y. Harabuchi, Y. Ono, T. Taketsugu, and K. Morokuma, Int. J. Quantum Chem. **115**, 258 (2015).
[16]Y. Harabuchi, A. Nakayama, and T. Taketsugu, Comput. Theor. Chem. **1000**, 70 (2012).
[17]H. Metiu, J. Ross, R. Silbey, and T. F. George, J. Chem. Phys. **61**, 3200 (1974).
[18]A. Tachibana, I. Okazaki, M. Koizumi, K. Hori, and T. Yamabe, J. Am. Chem. Soc. **107**, 1190 (1985).
[19]M. V. Basilevsky, Theor. Chim. Acta **72**, 63 (1987).
[20]W. Quapp, J. Mol. Struct. **695**, 95 (2004).
[21]J. M. Bofill and W. Quapp, J. Math. Chem. **51**, 1099 (2013).
[22]W. Quapp, Theor. Chim. Acta **75**, 447 (1989).
[23]T. Taketsugu and T. Hirano, J. Chem. Phys. **99**, 9806 (1993).
[24]T. Taketsugu and T. Hirano, J. Mol. Struct.: THEOCHEM **116**, 169 (1994).
[25]H. B. Schlegel, J. Chem. Soc., Faraday Trans. **90**, 1569 (1994).
[26]G. N. Sastry and S. Shaik, J. Phys. Chem. **100**, 12241 (1996).
[27]S. Shaik, D. Danovich, G. N. Sastry, P. Y. Ayala, and H. B. Schlegel, J. Am. Chem. Soc. **119**, 9237 (1997).
[28]H. Yamataka, M. Aida, and M. Dupuis, Chem. Phys. Lett. **300**, 583 (1999).
[29]Y. Kumeda and T. Taketsugu, J. Chem. Phys. **113**, 477 (2000).
[30]T. Taketsugu and Y. Kumeda, J. Chem. Phys. **114**, 6973 (2001).
[31]J. Li, X. S. Li, S. Shaik, and H. B. Schlegel, J. Phys. Chem. A **108**, 8526 (2004).
[32]J. Li, S. Shaik, and H. B. Schlegel, J. Phys. Chem. A **110**, 2801 (2006).
[33]J. M. Ramirez-Anguita, R. Gelabert, A. Gonzalez-Lafont, M. Moreno, and J. M. Lluch, Theor. Chem. Acc. **128**, 569 (2011).
[34]Y. Harabuchi and T. Taketsugu, Theor. Chem. Acc. **130**, 305 (2011).
[35]M. Haruta, T. Kobayashi, H. Sano, and N. Yamada, Chem. Lett. **16**, 405 (1987).
[36]M. Gao, A. Lyalin, and T. Taketsugu, Int. J. Quantum Chem. **113**, 443 (2013).
[37]M. Gao, A. Lyalin, and T. Taketsugu, J. Chem. Phys. **138**, 034701 (2013).
[38]M. Gao, A. Lyalin, S. Maeda, and T. Taketsugu, J. Chem. Theory Comput. **10**, 1623 (2014).
[39]W. H. Miller, N. C. Handy, and J. E. Adams, J. Chem. Phys. **72**, 99 (1980).
[40]S. Kato and K. Morokuma, J. Chem. Phys. **73**, 3900 (1980).
[41]M. J. Frisch, G. W. Trucks, H. B. Schlegel, G. E. Scuseria, M. A. Robb *et al.*, GAUSSIAN 09, Revision D.01, Gaussian, Inc., Wallingford, CT, 2009.
[42]S. Maeda, Y. Osada, K. Morokuma, and K. Ohno, GRRM11, version 11.01, 2011.
[43]S. Maeda, Y. Osada, Y. Harabuchi, T. Taketsugu, K. Morokuma *et al.*, GRRM, a developmental version at Hokkaido University, Sapporo, Japan, 2015.
[44]Y. Harabuchi, M. Okai, R. Yamamoto, Y. Ono, and T. Taketsugu, SPPR, a developmental version at Hokkaido University, Sapporo, Japan, 2015.
[45]P. Pyykkö, Angew. Chem., Int. Ed. **43**, 4412 (2004).